PHYSICAL REVIEW B **71**, 184308 (2005)

Nonlocal electron-phonon correlations in a dispersive Holstein model

Marco Zoli*
Istituto Nazionale Fisica della Materia, Dipartimento di Fisica, Universitá di Camerino, 62032, Italy

(Received 16 September 2004; published 27 May 2005)

Due to the dispersion of optical phonons, long range electron-phonon (*e-ph*) correlations renormalize downwards the coupling strength in the Holstein model. We evaluate the size of this effect both in a linear chain and in a square lattice for a time averaged *e-ph* potential, where the time variable is introduced according to the Matsubara formalism. Mapping the Holstein Hamiltonian onto the time scale we derive the perturbing source current which appears to be nontime retarded. This property permits to disentangle phonon and electron coordinates in the general path integral for an electron coupled to dispersive phonons. While the phonon paths can be integrated out analytically, the electron path integrations have to be done numerically. The equilibrium thermodynamic properties of the model are thus obtained as a function of the electron hopping value and of the phonon spectrum parameters. We derive the *e-ph* corrections to the phonon free energy and show that its temperature derivatives do not depend on the *e-ph* effective coupling, hence, the Holstein phonon heat capacity is strictly harmonic. A significant upturn in the low temperature total heat capacity over *T* ratio is attributed to the electron hopping which largely contributes to the action.

DOI: 10.1103/PhysRevB.71.184308 PACS number(s): 63.20.Kr, 31.15.Kb, 65.40.Ba

I. INTRODUCTION

Theoretical investigation on the effects of nonlocality in electron-phonon (*e-ph*) coupling[1,2] has grown considerably during the last years in conjunction with the large interest for organic molecular crystals,[3] carbon nanotubes,[4,5] and conducting polymers exhibiting polaronic properties. In the Su-Schrieffer-Heeger (SSH) Hamiltonian[6] the electronic hopping is accompanied by a relative displacement between adjacent atomic sites that causes a nonlocal *e-ph* coupling with vertex function depending both on the electronic and the phononic wave vector. This feature leads to peculiar static and dynamical properties[7] for the SSH model which also displays dimension dependent mass behavior for the acoustical polarons.[8,9] In a path integral investigation of the equilibrium thermodynamics we have shown[10] that the purely electronic hopping dominates the low temperature thermodynamics as it is responsible for a characteristic upturn in the heat capacity over *T* ratio pointing to a glassylike behavior in the one dimensional chain. Moreover, phonon anharmonicities induced by *e-ph* interactions can be large in the SSH model due to the time retarded nature of the perturbing source current.[11]

In the Holstein model, the coupling of electrons to dispersionless optical phonons is essentially local and the electronic energy at a lattice site linearly depends on the atomic displacement at that site.[12] Thus, in the strong coupling regime, the unit comprising electron plus induced lattice deformation is generally a small object (on the lattice scale) undergoing a sizeable mass renormalization. Large adiabaticities may, however, induce a spread in the real space for the Holstein polaron which accordingly becomes lighter. This effect is more pronounced in higher dimensionality.[13] On the other hand, the dispersive nature of the phonon spectrum is recognized as a fundamental feature of the Holstein model as it allows for finite values of the electronic site jump probability while a dispersionless model would lead to unphysical divergences.[12,14] Also ground state properties such as electron bandwidth and effective mass are more properly evaluated versus dimensionality within a dispersive model. In this paper we investigate to which extent the realistic assumption of dispersive phonons may induce nonlocal correlations which consistently renormalize the effective *e-ph* coupling both in one and two dimensions. We emphasize that the model and the results hereafter presented, being valid for any coupling strength, are independent of the existence of small polarons in the system.

Unlike the SSH model, the Holstein electron hopping does not induce a shift in the atomic displacement. Thus the perturbing *e-ph* current does not depend on the electronic paths and, along the time scale, it turns out to be intrinsically local. Applying space-time mapping techniques[15] we show that this feature allows an elegant path integral formulation[16] of the Holstein partition function in which electron and dispersive phonon coordinates appear to be decoupled. Section II outlines the Hamiltonian model while the path integral method is described in Sec. III. The results of our work are reported on in Sec. IV and some final remarks are given in Sec. V.

II. THE DISPERSIVE HOLSTEIN MODEL

We consider the dimension dependent Holstein Hamiltonian consisting of: (i) one electron hopping term, (ii) an interaction which couples the electronic density ($f^\dagger_{\mathbf{l}} f_{\mathbf{l}}$) to the phonon creation ($b^\dagger_{\mathbf{l}}$) and annihilation ($b_{\mathbf{l}}$) operators at a given site $\mathbf{l}$, (iii) dispersive harmonic optical phonons

$$H = H^{e} + H^{e\text{-}ph} + H^{ph},$$

$$H^{e} = -t \sum_{\langle \mathbf{l},\mathbf{m} \rangle} f^\dagger_{\mathbf{l}} f_{\mathbf{m}},$$

©2005 The American Physical Society

$$H^{e\text{-}ph} = g\sum_{\mathbf{l}} f_{\mathbf{l}}^{\dagger} f_{\mathbf{l}} (b_{\mathbf{l}}^{\dagger} + b_{\mathbf{l}}),$$

$$H^{ph} = \sum_{\mathbf{q}} \omega(\mathbf{q}) b_{\mathbf{q}}^{\dagger} b_{\mathbf{q}}, \tag{1}$$

the first sum is over z nearest neighbors, t is the tight binding overlap integral. $b_{\mathbf{q}}^{\dagger}$ is the Fourier transform of $b_{\mathbf{l}}^{\dagger}$ and $\omega(\mathbf{q})$ is the frequency of the phonon with vector momentum $\mathbf{q}$. g is the *e-ph* coupling in energy units.

The phonons operators can be written in terms of the isotropic displacement field $u_{\mathbf{n}}$ as

$$b_{\mathbf{l}}^{\dagger} + b_{\mathbf{l}} = \frac{1}{N}\sum_{\mathbf{q}} \sqrt{2M\omega(\mathbf{q})} \sum_{\mathbf{n}} \exp[i\mathbf{q}\cdot(\mathbf{l}-\mathbf{n})]u_{\mathbf{n}}, \tag{2}$$

where M is the atomic mass. Then, the *e-ph* term in (1) transforms as follows:

$$H^{e\text{-}ph} = \frac{g}{N}\sum_{\mathbf{q}} \sqrt{2M\omega(\mathbf{q})} \sum_{\mathbf{l},\mathbf{n}} f_{\mathbf{l}}^{\dagger} f_{\mathbf{l}} u_{\mathbf{n}} \exp[i\mathbf{q}\cdot(\mathbf{l}-\mathbf{n})]. \tag{3}$$

The sum over $\mathbf{n}$ spans all nth neighbors sites of the $\mathbf{l}$ lattice site in any dimensionality. Thus, although the Holstein Hamiltonian assumes a local *e-ph* interaction, the dispersive nature of the phonon spectrum clearly introduces *e-ph* real space correlations which renormalize the dimension dependent effective coupling. Fourier transforming the atomic displacement field and taking the lattice constant $|\mathbf{a}|=1$, from Eq. (3) we obtain for a linear chain and a square lattice, respectively,

$$H_d^{e\text{-}ph} = \frac{g}{N^{3/2}}\sum_{\mathbf{l}} f_{\mathbf{l}}^{\dagger} f_{\mathbf{l}} \sum_{\mathbf{q},\mathbf{q}'} \sqrt{2M\omega(\mathbf{q})} \exp(i\mathbf{q}'\cdot\mathbf{l}) \times u_{\mathbf{q}'} S_d(\mathbf{q}'-\mathbf{q}),$$

$$S_{1D}(q'-q) \equiv 1 + 2\sum_{n=1}^{n^*} \cos[n(q'-q)],$$

$$\begin{aligned} S_{2D}(\mathbf{q}'-\mathbf{q}) \equiv{}& 1 + 2\sum_{n=1}^{n^*} [\cos n(q_x'-q_x) + \cos n(q_y'-q_y)] \\ &+ 2\sum_{m,n=1}^{n^*} \{\cos[m(q_x'-q_x) + n(q_y'-q_y)] \\ &+ \cos[m(q_x'-q_x) - n(q_y'-q_y)]\}. \end{aligned} \tag{4}$$

While, in principle, the sum over n should cover all the N sites in the lattice we introduce the cutoff n^* which will allow us to monitor the behavior of the coupling as a function of the range of the *e-ph* correlations. Note that in one dimension (1D), the integer n numbers the neighbors shells up to n^* while in two dimensions (2D), the $n^*=1$ term includes the second neighbors shell, the sum up to $n^*=2$ includes the fifth neighbors shells, $n^*=3$ covers the nineth shell and so on. Switching off the interatomic forces, $\omega(\mathbf{q})=\omega_0$, one would recover from (4) a local *e-ph* coupling model with $S_d\equiv 1$. As no approximation has been done at this stage Eqs. (4) are general.

Taking into account first neighbors intermolecular forces in the Holstein molecular crystal model, the optical phonon spectra are given in 1D and 2D, respectively, by[14]

$$\omega_{1D}^2(q) = \omega_0^2/2 + \omega_1^2 + \sqrt{\omega_0^4/4 + \omega_0^2\omega_1^2\cos q + \omega_1^4},$$

$$\omega_{2D}^2(\mathbf{q}) = \omega_0^2/2 + 2\omega_1^2 + \sqrt{\omega_0^4/4 + \omega_0^2\omega_1^2 g(\mathbf{q}) + \omega_1^4[2+h(\mathbf{q})]},$$

$$g(\mathbf{q}) = \cos q_x + \cos q_y,$$

$$h(\mathbf{q}) = 2\cos(q_x - q_y), \tag{5}$$

where ω_0 and ω_1 are the intramolecular and intermolecular energies, respectively.

Treating in (4) the phonon coordinates as classical variables interacting with quantum mechanical Fermion operators we assume a semiclassical version of the dispersive Holstein Hamiltonian. This is the main approximation in the model which will permit us to derive a time dependent source current for the general electron path integral. Averaging (4) on the electronic ground state we also define the *e-ph* energy per lattice site

$$\frac{\langle H_d^{e\text{-}ph}\rangle}{N} = \sum_{\mathbf{q}} \langle H_d^{e\text{-}ph}\rangle_{\mathbf{q}},$$

$$\langle H_d^{e\text{-}ph}\rangle_{\mathbf{q}} = \frac{g}{N^{3/2}}\sqrt{2M\omega(\mathbf{q})}\sum_{\mathbf{q}'} \rho_{\mathbf{q}'} u_{\mathbf{q}'} S_d(\mathbf{q}'-\mathbf{q}),$$

$$\rho_{\mathbf{q}'} = \frac{1}{N}\sum_{\mathbf{l}} \langle f_{\mathbf{l}}^{\dagger} f_{\mathbf{l}}\rangle \exp(i\mathbf{q}'\cdot\mathbf{l}), \tag{6}$$

which will be used in the next section.

While we are thus neglecting the quantum nature of the lattice vibrations, the latter may in itself lead to retardation effects in the ground state structure of the composite quasiparticle made of one electron plus phonon excitations in the adiabatic regime. Moreover, at finite temperatures, the quantum lattice fluctuations are expected to influence the thermodynamics of the system mainly for intermediate values of the *e-ph* coupling.[17]

III. THE PATH INTEGRAL METHOD

Let us apply to the Holstein Hamiltonian space-time mapping techniques[15,18] which allow us to write the general path integral for one electron particle in a bath of dispersive phonons. Thus we introduce $\mathbf{x}(\tau)$ and $\mathbf{y}(\tau')$ as the electron coordinates at the $\mathbf{l}$ and $\mathbf{m}$ lattice sites respectively, and H^e in (1) transforms into

$$H^e(\tau,\tau') = -t\{f^{\dagger}[\mathbf{x}(\tau)]f[\mathbf{y}(\tau')] + f^{\dagger}[\mathbf{y}(\tau')]f[\mathbf{x}(\tau)]\}. \tag{7}$$

τ and τ' are continuous variables ($\in[0,\beta]$) in the Matsubara Green's functions formalism with β being the inverse temperature, hence, the electron hops are not constrained to first neighbors sites. Accordingly, Eq. (7) is more general than H^e

in (1). After setting $\tau'=0$, $\mathbf{y}(0)\equiv 0$, we take the thermal averages for the electron operators over the ground state of the Hamiltonian thus obtaining in d dimensions the average energy per lattice site due to electron hopping

$$h^e(\tau)\equiv\frac{\langle H^e(\tau)\rangle}{N}=-t\{G[-\mathbf{x}(\tau),-\tau]+G[\mathbf{x}(\tau),\tau]\},$$

$$G[\mathbf{x}(\tau),\tau]=\frac{1}{\beta}\int\frac{d\mathbf{k}}{\pi^d}\exp[i\mathbf{k}\cdot\mathbf{x}(\tau)]\sum_n\frac{\exp(-i\hbar\nu_n\tau)}{i\hbar\nu_n-\epsilon_{\mathbf{k}}}. \quad (8)$$

ν_n are the fermionic Matsubara frequencies and $\epsilon_{\mathbf{k}}=-2t\Sigma_{i=x,y,z}\cos(k_i)$ is the electron dispersion relation.

The spatial *e-ph* correlations contained in (3) are mapped onto the time axis introducing the τ dependence in the displacement field: $u_{\mathbf{q}}\rightarrow u_{\mathbf{q}}(\tau)$. Assuming periodic atomic particle paths: $u_{\mathbf{q}}(\tau+\beta)=u_{\mathbf{q}}(\tau)$ we can expand $u_{\mathbf{q}}(\tau)$ in N_F Fourier components

$$u_{\mathbf{q}}(\tau)=u_0+\sum_{n=1}^{N_F}2[(\Re u_n)_{\mathbf{q}}\cos(\omega_n\tau)-(\Im u_n)_{\mathbf{q}}\sin(\omega_n\tau)] \quad (9)$$

with $\omega_n=2n\pi/\beta$.

Then, on the basis of Eqs. (6) and (9), we identify the perturbing source current of the Holstein model with the τ dependent averaged *e-ph* Hamiltonian term

$$j(\tau)=\sum_{\mathbf{q}}j_{\mathbf{q}}(\tau),$$

$$j_{\mathbf{q}}(\tau)=\frac{g}{N^{3/2}}\sqrt{2M\omega(\mathbf{q})}\sum_{\mathbf{q}'}u_{\mathbf{q}'}(\tau)\rho_{\mathbf{q}'}S_d(\mathbf{q}'-\mathbf{q}). \quad (10)$$

With these premises, we are now in the position to write the general path integral[19] for an Holstein electron in a bath of dispersive phonons. Assuming a mixed representation, the electron paths are taken in real space while the phonon paths are in momentum space. The electron path integral reads

$$\langle\mathbf{x}(\beta)|\mathbf{x}(0)\rangle=\prod_{\mathbf{q}}\langle\mathbf{x}(\beta)|\mathbf{x}(0)\rangle_{\mathbf{q}},$$

$$\begin{aligned}\langle\mathbf{x}(\beta)|\mathbf{x}(0)\rangle_{\mathbf{q}}=\int Du_{\mathbf{q}}(\tau)\exp\Bigg\{-\int_0^\beta d\tau\frac{M}{2}[\dot{u}_{\mathbf{q}}{}^2(\tau)\\+\omega^2(\mathbf{q})u_{\mathbf{q}}^2(\tau)]\Bigg\}\int D\mathbf{x}(\tau)\\\times\exp\Bigg\{-\int_0^\beta d\tau\Bigg[\frac{m}{2}\dot{\mathbf{x}}^2(\tau)+h^e(\tau)-j_{\mathbf{q}}(\tau)\Bigg]\Bigg\},\end{aligned} \quad (11)$$

where the kinetic term (m is the electron mass) is normalized by the functional measure of integration over the electron paths.

As a direct consequence of the time-local nature of the *e-ph* interactions, the Holstein source current does not depend on the electron path coordinates. Then $j_{\mathbf{q}}(\tau)$ in (11) can be easily integrated over τ using Eqs. (9) and (10) and noticing that

$$\int_0^\beta u_{\mathbf{q}}(\tau)=\frac{\beta u_0}{\sqrt{N}}, \quad (12)$$

we get

$$\int_0^\beta d\tau j_{\mathbf{q}}(\tau)=\beta u_0 g_d(\mathbf{q}),$$

$$g_d(\mathbf{q})=\frac{g}{N^2}\sqrt{2M\omega(\mathbf{q})}\sum_{\mathbf{q}'}\rho_{\mathbf{q}'}S_d(\mathbf{q}'-\mathbf{q}). \quad (13)$$

$g_d(\mathbf{q})$ is thus a time averaged *e-ph* potential.

The total partition function can be derived from (11) by imposing the closure condition both on the phonons [Eq. (9)] and on the electron paths, $\mathbf{x}(\beta)=\mathbf{x}(0)$. Using (13), we obtain

$$\begin{aligned}Z_T=\prod_{\mathbf{q}}\oint Du_{\mathbf{q}}(\tau)\exp\Bigg\{\beta u_0 g_d(\mathbf{q})-\int_0^\beta d\tau\frac{M}{2}[\dot{u}_{\mathbf{q}}{}^2(\tau)\\+\omega_{\mathbf{q}}^2u_{\mathbf{q}}^2(\tau)]\Bigg\}\times\oint D\mathbf{x}(\tau)\exp\Bigg\{-\int_0^\beta d\tau\Bigg[\frac{m}{2}\dot{\mathbf{x}}^2(\tau)\\+h^e(\tau)\Bigg]\Bigg\}.\end{aligned} \quad (14)$$

Equation (14) shows that the averaged *e-ph* coupling is weighed only by the τ-independent component u_0 of the displacement field. This property will prove to be essential in the next calculations. The integration over the phonon paths can be done analytically choosing a measure of integration which normalizes the kinetic term in the phonon field action

$$\begin{aligned}\oint Du_{\mathbf{q}}(\tau)\equiv\frac{\sqrt{2}}{(2\lambda_M)^{(2N_F+1)}}\int_{-\infty}^{\infty}du_0\\\times\prod_{n=1}^{N_F}(2\pi n)^2\int_{-\infty}^{\infty}d(\Re u_n)_{\mathbf{q}}\int_{-\infty}^{\infty}d(\Im u_n)_{\mathbf{q}}\\\oint Du_{\mathbf{q}}(\tau)\exp\Bigg[-\frac{M}{2}\int_0^\beta d\tau\dot{u}_{\mathbf{q}}{}^2(\tau)\Bigg]\equiv 1\end{aligned} \quad (15)$$

being $\lambda_M=\sqrt{\pi\hbar^2\beta/M}$. In the following calculations we set $M\sim 10^4$ m.

Using the result[20]

$$\int_{-\infty}^{\infty}du_0\exp(bu_0-cu_0^2)=\sqrt{\frac{\pi}{c}}\exp(b^2/4c), \quad (16)$$

we derive

$$Z_T = \prod_q P(\mathbf{q}) \times \oint D\mathbf{x}(\tau)\exp\left\{-\int_0^\beta d\tau\left[\frac{m}{2}\dot{\mathbf{x}}^2(\tau) + h^e(\tau)\right]\right\},$$

$$P(\mathbf{q}) = \frac{1}{\beta\omega(\mathbf{q})}\exp\left\{\frac{[g_d(\mathbf{q})\lambda_M]^2}{2\pi\omega(\mathbf{q})^2}\right\}\prod_{n=1}^{N_F}\frac{(2n\pi)^2}{(2n\pi)^2 + [\beta\omega(\mathbf{q})]^2}. \tag{17}$$

Equation (17) represents the main analytical result of our model. The exponential function in $P(\mathbf{q})$ embodies the effect of the nonlocal correlations due to the dispersive nature of the phonon spectrum. Phonon and electron contributions to the partition function are decoupled although the effective potential $g_d(\mathbf{q})$ carries a dependence on the electron density profile in momentum space through the function $\rho(\mathbf{q})$.

IV. ELECTRON-PHONON CORRELATIONS AND THERMODYNAMICAL RESULTS

First we analyze the behavior of the time (temperature) averaged *e-ph* potential [Eq. (13)] in the case of a linear chain and of a square lattice.

Note that $u_{\mathbf{q}}(\tau)$ in (9) is a real quantity consistently with the closure condition on the lattice displacement path. Accordingly, from (6) [and (10)], we take a real profile also for the electron distribution in momentum space. Setting the total electron density on a single site and defining ρ_0 as the on site electron density, from (6), we write the electron profile $\rho_q = \rho_0\cos(q)$ for the 1D system and $\rho_{\mathbf{q}} = \rho_0\cos(q_x)\cos(q_y)$ for the 2D system. Since the momentum integration runs over $q_i \in [0, \pi/2]$, ρ_0 represents in both cases the total electron density. This choice is convenient in order to normalize the averaged *e-ph* couplings over the same parameter both in 1D and 2D. Physically it corresponds to pin one electron on a lattice site and to measure the effects on the potential due to the *e-ph* correlations with variable range.

Let us assume low energy phonon spectra parameters, $\omega_0 = 20$ meV and $\omega_1 = 10$ meV. Setting $g = 3$, we take a strong bare Holstein coupling g although the general trend of our results holds for any value of g. In Fig. 1(a), $g_{1D}(q)/\rho_0$ is plotted for three choices of the cutoff n^* [see Eqs. (4)] to emphasize the dependence of the potential on the *e-ph* interaction range. The constant value of the potential obtained for $\omega_1 = 0$ is also reported on. While in the case of short correlations ($n^* = 4$) there is a range of wave vectors in which the effective coupling becomes larger than the dispersionless coupling, long range *e-ph* correlations substantially reduce the effective potential with respect to the dispersionless case and set in an oscillating behavior which makes the renormalization q dependent. The potential tends to converge for the value $n^* = 24$ which corresponds to 48 lattice sites along the chain.

The projections of the two dimensional *e-ph* potential along the y component of the wave vector is reported on in Fig. 1(b) for three values of the cutoff on the correlation range. For $n^* = 1$ the correlation range is extended to the second neighbor shell thus including eight lattice sites. For $n^* = 2$ and $n^* = 3$ we normalize over 24 and 48 lattice sites, respectively. Then, the three values of n^* in 2D span as many lattice sites as the three values of n^* in 1D, respectively. This choice permits to normalize consistently the potential for the linear chain and the square lattice. There is a strong renormalization for the 2D effective potential with respect to the dispersionless case for any value of the wave vector. By extending the correlation range this tendency becomes more pronounced for q_y close to the center and to the edge of the reduced Brillouin zone. An analogous behavior is found by projecting the 2D potential along the q_x axis. The 2D potential stabilizes by including the ninth neighbor shell ($n^* = 3$) in the correlation range.

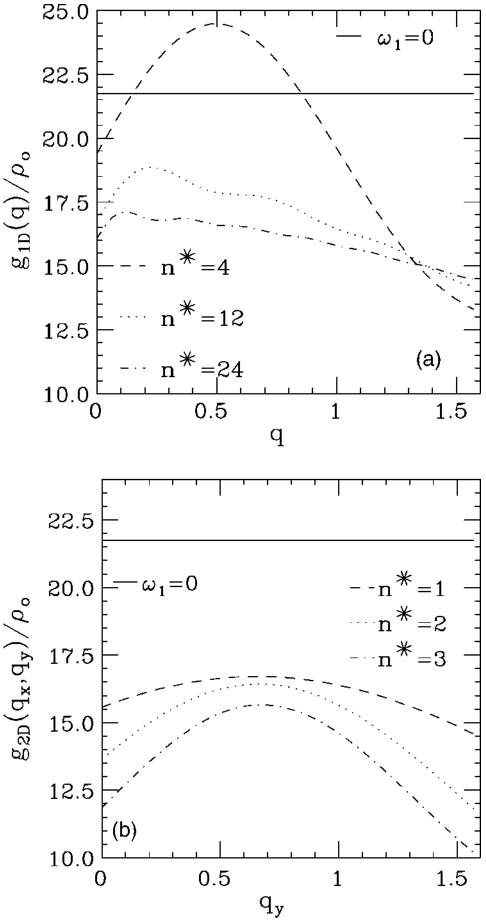

FIG. 1. (a) Temperature averaged *e-ph* coupling (in units meV Å^{-1} vs wave vector for a linear chain. n^* represents the cutoff on the *e-ph* correlations. ρ_0 is the electron density. $\omega_0 = 20$ meV and $\omega_1 = 10$ meV. $g = 3$. The dispersionless *e-ph* coupling is obtained for $\omega_0 = 0$. (b) Temperature averaged *e-ph* coupling in two dimensions vs the y component of the momentum. The cases $n^* = 1$, $n^* = 2$, and $n^* = 3$ imply that the correlation range includes the second, the fifth, and the ninth neighbors shell, respectively. The input parameters are as in (a).

Then, an increased range for the *e-ph* correlations leads to an effect which is qualitatively analogous to that one would get by hardening the phonon spectrum: a reduction of the effective coupling and the consequent lightening of the quasiparticle effective mass.[21]

Let us see now to which extent the momentum dependent potential affects the thermodynamics of the system. In

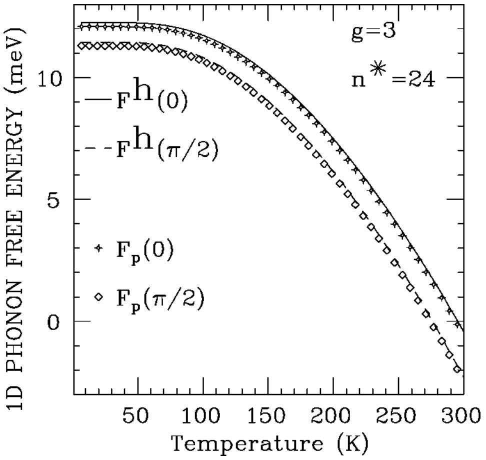

FIG. 2. Anharmonic F_p and harmonic F^h phonon free energies for two values of the one dimensional wave vector $q=0,\pi/2$. The phonon spectrum parameters are as in Fig. 1(a).

the total partition function [Eq. (14)] the electronic and phononic paths have been integrated out separately as the source current does not depend on the electronic coordinates. The **q**-phonon contribution to the partition function is thus given by $P(\mathbf{q})$ in (17), hence, the free energy due to the **q** mode is

$$F_p(\mathbf{q}) = \frac{1}{\beta}\ln[\beta\omega(\mathbf{q})] - \frac{1}{\beta}\ln\left\{\prod_{n=1}^{N_F}\frac{(2n\pi)^2}{(2n\pi)^2+[\beta\omega(\mathbf{q})]^2}\right\} - \frac{[g_d(\mathbf{q})\hbar]^2}{2M\omega(\mathbf{q})^2}, \tag{18}$$

where the first two terms represent the harmonic free energy $F^h(\mathbf{q})$. Since $F^h(\mathbf{q})=\beta^{-1}\ln\{2\sinh[\beta\omega(\mathbf{q})/2]\}$ we find a constraint which allows us to determine the cutoff $N_F=N_F[\omega(\mathbf{q}),T]$. For the 1D system, at $T=1$ K and for the phonon parameters given above, we get $N_F \sim c10^7$ with c varying in the range (4.2–4.5) according to the q mode.

The *e-ph* interactions renormalize downwards the harmonic values for any **q** as $F_p(\mathbf{q})-F^h(\mathbf{q}) \propto -g^2(\mathbf{q})/\omega^2(\mathbf{q})$ but the temperature derivatives of the free energy do not involve the coupling term. Then, on general grounds, phonon entropy and heat capacity are not affected by the strength of the *e-ph* interaction and signatures of *e-ph* anharmonicity should not be expected in the equilibrium properties of the phonon subsystem. This is a direct macroscopic effect of the local nature of the interactions in the Holstein model. On the other hand, lattice nonlinearities may appear in the ground state properties of the Holstein Hamiltonian and significantly modify the dynamical properties of the polaronic quasiparticles.[22,23]

In Fig. 2, we consider the linear chain with the cutoff $n^*=24$ of Fig. 1(a) and set $\rho_0=1$. The phonon free energies are plotted for two selected wave vectors together with the corresponding harmonic values. It is seen that the renormalization of the q-dependent free energies due to the *e-ph* coupling is very weak. However, being $g^2(\mathbf{q})/\omega^2(\mathbf{q}) \propto g^2/\omega(\mathbf{q})$, the phonon free energy reduction may be appreciable in very low energy phonon spectra provided that the bare coupling g is sufficiently strong.

Next we turn to the evaluation of the electronic contribution to the total partition function [Eq. (17)]. The results hereafter presented refer to the case of 1D electronic paths. As the hopping energy density is related to the electron propagator [Eq. (8)] a preliminar wave vector integration prepares h^e as a function of the path coordinates. Then, the $\oint Dx(\tau)$ integration has to be done numerically. Assuming the periodicity condition $x(\tau)=x(\tau+\beta)$, the particle paths can be expanded in N_p Fourier components

$$x(\tau) \sim x_0 + \sum_{n=1}^{N_p} 2[\Re x_n \cos(\xi_n\tau) - \Im x_n \sin(\xi_n\tau)],$$

$$\xi_n = 2\pi n/\beta \tag{19}$$

so that the functional measure of integration

$$\oint Dx(\tau) \sim \frac{\sqrt{2}}{(2\lambda_m)^{(2N_p+1)}}\int_{-\Lambda}^{\Lambda} dx_0 \prod_{n=1}^{N_p}(2\pi n)^2 \times \int_{-2\Lambda}^{2\Lambda} d\Re x_n \int_{-2\Lambda}^{2\Lambda} d\Im x_n,$$

$$\lambda_m = \sqrt{\pi\hbar^2\beta/m} \tag{20}$$

normalizes the free electron term in (17),

$$\oint D\mathbf{x}(\tau)\exp\left[-\int_0^\beta d\tau \frac{m}{2}\dot{\mathbf{x}}^2(\tau)\right] = 1. \tag{21}$$

Equation (21) provides a criterion to set the cutoff Λ which turns out to be $\propto \lambda_m$ thus implying that the maximum amplitude of the particle path coefficients becomes large in the low temperature range. This is consistent with the physical expectation that towards high temperatures only a reduced number of paths contributes to the action which thus tends to the classical limit. Accordingly, the integration over each Fourier component in (20) is carried out over a number of points $N_\Lambda \propto K/\sqrt{T}$ and the electron hopping in the path integral (18) is weighed over a total number of electron paths $(N_\Lambda+1)^{2N_p+1}$. We find that $K \sim 20$ and $N_p=2$ suffice to ensure numerical convergence. While the free electron term only scarcely contributes to the electronic action, the hopping dependent action is dominant also at low temperatures. In fact, according to our measure of integration, the ensemble of relevant particle paths (over which the hopping energy density is evaluated) is T dependent. However, given a single set of path parameters one can monitor the h^e behavior versus T. It turns out that the hopping decreases by decreasing T but its value remains appreciable also at low temperatures. Since the $d\tau$ integration range is larger at lower temperatures, the overall hopping contribution to the total action is relevant also at low T.

The equilibrium thermodynamics of the Holstein model can be derived from (17). We average the phonon contribution over a set of 50 modes in the 1D Brillouin zone and take the bare *e-ph* coupling $g=3$. Phonon and electron free ener-

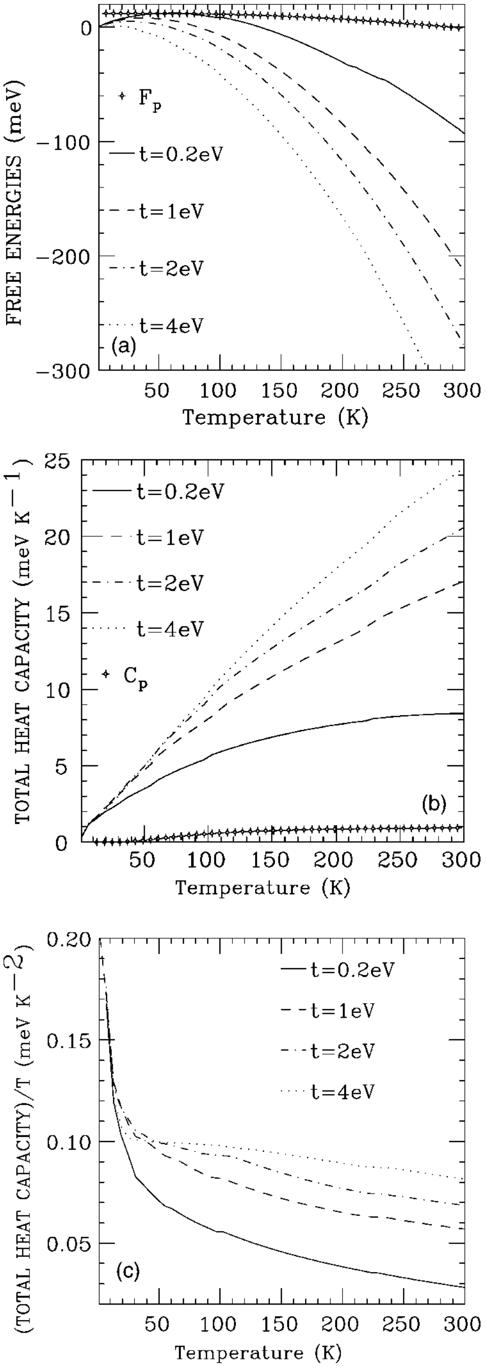

FIG. 3. (a) Phonon free energy (symbols) and electron free energies for four values of the hopping integral t. The phonon energies and the *e-ph* coupling are as in Figs. 1. (b) Total (electron plus phonon) heat capacities for four values of t. The phonon heat capacity is plotted separately. (c) Total heat capacities over temperature ratio.

gies are plotted separately versus temperature in Fig. 3(a). Note that in the low T range the electron free energy has a positive derivative both for narrow and wide band values although the range shrinks by increasing the hopping integral value. For $t=0.2$ eV, the electron free energy gets the maximum at $T\sim 60$ K while for $t=4$ eV, the maximum occurs at $T\sim 13$ K. This feature is mirrored in the total heat capacity which is reported on in Fig. 3(b) for four t values together with the phonon heat capacity normalized over the number of modes. As noted above the latter overlaps the purely harmonic heat capacity no matter how large the *e-ph* coupling may be. Thus the Holstein phonon heat capacity does not contain signatures of *e-ph* anharmonicity. The total heat capacity over T ratio shows an upturn at low temperatures as shown in Fig. 3(c) due to the electron hopping mechanism which has already been encountered in the study of the SSH model.[11] However, while in the latter the shape of the low T upturn could be tuned by the strength of the *e-ph* coupling in the source action, in the Holstein model the low T anomaly has purely electronic origins as the *e-ph* effects are contained in the phonon partition function. This also explains why the absolute values of the Holstein heat capacity are much lower than the SSH heat capacity throughout the whole temperature range.

V. CONCLUSIONS

In the Holstein model, the *e-ph* coupling is local and the vertex function does not depend on the wave vectors. Nonetheless nonlocal *e-ph* correlations arise in the system once the dispersive nature of the phonon spectrum is taken into account. I have studied a semiclassical version of the one electron Holstein Hamiltonian in which quantum mechanical fermion operators interact with classical lattice displacements. Applying the path integral method the real space interactions can be mapped onto the time scale and, in the Matsubara formalism, we have derived an analytical expression for the time averaged wave vector dependent *e-ph* coupling. Assuming a force constant intermolecular model we have evaluated the renormalization of the wave vector dependent *e-ph* coupling, both in one and two dimensions, as a function of the range of the *e-ph* correlations. In 1D, for short range correlations ($n^*=4$), I find an enhancement of the effective coupling with respect to the dispersionless coupling in a window of phonon wave vectors. By increasing n^*, the effective coupling renormalizes downwards for any q although the reduction is larger towards the edge of the Brillouin zone. In 2D, the renormalization is even more pronounced and takes place also for small values of the cutoff on the correlation range.

Thus, the inclusion of the *e-ph* correlations in the effective coupling has an effect which is similar to that one would obtain by enhancing the characteristic phonon frequency and it ultimately leads to reduce the effective mass of the quasiparticle. The Holstein polaron mass in a dispersive phonon model is thus lighter than in a dispersionless model.

Mapping the *e-ph* interaction onto the time scale we also find that the perturbing source current of the model depends on the time only through the atomic displacement field, hence, it is not retarded. Then, the temperature (time) averaged current is proportional to the averaged atomic displacement and it does not include the electronic coordinates. This property allows us to decouple phonon and electron degrees of freedom in the general path integral and in the total partition function. Such a disentanglement does not occur in the Su-Schrieffer-Heeger model[10] as the source current does depend on the electron path coordinates. As a physical consequence the renormalized Holstein *e-ph* coupling is frozen in the phonon partition function while the electron action is dominated by the hopping energy density. After integrating out analytically the phonon degrees of freedom we have obtained the **q**-dependent phonon free energy and estimated the *e-ph* corrections (with respect to the harmonic values) in the thermodynamical properties. It turns out that the Holstein heat capacity does not show any signature of phonon anharmonicity induced by the *e-ph* interactions. This marks a striking difference with respect to the thermodynamical behavior of the previously investigated Su-Schrieffer-Heeger model. On the other hand, the electron hopping energy strongly contributes to the total action of the Holstein model and, at low temperatures, it is responsible for a peculiar upturn in the *heat capacity over temperature* (C_V/T) ratio. While qualitatively the latter feature had also been envisaged in the SSH heat capacity, in the Holstein model the shape of the broad upturn has purely electronic origins and it is not affected by the *e-ph* source action. This explains why C_V/T has a negative temperature derivative throughout the whole T range for any value of the hopping integral.

ACKNOWLEDGMENTS

The author acknowledges Professor A. N. Das for fruitful discussions and a critical reading of the paper. This work is part of the Joint Research Project (Ph-T 4) under the Indo-Italian Programme of Co-operation in Science and Technology 2002–2004. I am thankful to Dr. G. Costantini for his effective collaboration.

---

*Email address: marco.zoli@unicam.it

[1] V. M. Stojanović, P. A. Bobbert, and M. A. J. Michels, Phys. Rev. B **69**, 144302 (2004).

[2] C. A. Perroni, E. Piegari, M. Capone, and V. Cataudella, Phys. Rev. B **69**, 174301 (2004).

[3] K. Hannewald, V. M. Stojanović, J. M. T. Schellekens, P. A. Bobbert, G. Kresse, and J. Hafner, Phys. Rev. B **69**, 075211 (2004).

[4] L. M. Woods and G. D. Mahan, Phys. Rev. B **61**, 10 651 (2000).

[5] M. Verissimo-Alves, R. B. Capaz, B. Koiller, E. Artacho, and H. Chacham, Phys. Rev. Lett. **86**, 3372 (2001).

[6] W. P. Su, J. R. Schrieffer, and A. J. Heeger, Phys. Rev. Lett. **42**, 1698 (1979); A. J. Heeger, S. Kivelson, J. R. Schrieffer, and W.-P. Su, Rev. Mod. Phys. **60**, 781 (1988).

[7] K. Michielsen and H. De Raedt, Z. Phys. B: Condens. Matter **103**, 391 (1997).

[8] N. Miyasaka and Y. Ono, J. Phys. Soc. Jpn. **70**, 2968 (2001).

[9] M. Zoli, Phys. Rev. B **66**, 012303 (2002).

[10] M. Zoli, Phys. Rev. B **67**, 195102 (2003).

[11] M. Zoli, Phys. Rev. B **70**, 184301 (2004).

[12] T. Holstein, Ann. Phys. (N.Y.) **8**, 325 (1959).

[13] M. Zoli and A. N. Das, J. Phys.: Condens. Matter **16**, 3597 (2004).

[14] M. Zoli, Phys. Rev. B **57**, 10 555 (1998).

[15] D. R. Hamann, Phys. Rev. B **2**, 1373 (1970).

[16] R. P. Feynman, Phys. Rev. **97**, 660 (1955).

[17] H. De Raedt and A. Lagendijk, Phys. Rev. B **27**, 6097 (1983).

[18] C. C. Yu and P. W. Anderson, Phys. Rev. B **29**, 6165 (1984).

[19] H. Kleinert, *Path Integrals in Quantum Mechanics, Statistics and Polymer Physics* (World Scientific, Singapore, 1995).

[20] I. S. Gradshteyn and I. M. Ryzhik, *Tables of Integrals, Series and Products* (Academic Press, New York, 1965).

[21] A. S. Alexandrov and P. E. Kornilovitch, Phys. Rev. Lett. **82**, 807 (1999).

[22] N. K. Voulgarakis and G. P. Tsironis, Phys. Rev. B **63**, 014302 (2001).

[23] Y. Zolotaryuk, P. L. Christiansen, and J. J. Rasmussen, Phys. Rev. B **58**, 14 305 (1998).